J|A|C|S
ARTICLES

Published on Web 11/17/2008

Synthesis and Characterization of Fluorescent Displacers for Online Monitoring of Displacement Chromatography

Christopher J. Morrison,[†] Sun Kyu Park,[‡] Chester Simocko,[‡] Scott A. McCallum,[§] Steven M. Cramer,*[,†] and J. A. Moore[‡]

Departments of Chemical and Biological Engineering and of Biology, Center for Biotechnology and Interdisciplinary Studies, and Department of Chemistry and Chemical Biology, Rensselaer Polytechnic Institute, 110 Eighth Street, Troy, New York 12180

Received August 8, 2008; E-mail: crames@rpi.edu

Abstract: One of the major impediments to the implementation of displacement chromatography for the purification of biomolecules is the need to collect fractions from the column effluent for time-consuming offline analysis. The ability to employ direct online monitoring of displacement chromatography would have significant implications for applications ranging from analytical to preparative bioseparations. To this end, a set of novel fluorescent displacers were rationally designed using known chemically selective displacers as a template. Fluorescent cores were functionalized with different charge moieties, creating a homologous library of displacers. These compounds were then tested on two protein pairs, α-chymotrypsinogen A/ribonuclease A and cytochrome *c*/lysozyme, using batch and column displacement experiments. Of the synthesized displacers, two were found to be highly selective while one was determined to be a high-affinity displacer. Column displacements using one of the selective displacers yielded complete separation of both protein pairs while facilitating direct online detection using UV and fluorescence detection. Saturation transfer difference NMR was also carried out to investigate the binding of the fluorescent displacers to proteins. The results indicated a selective binding between the selective displacers and α-chymotrypsinogen A, while no binding was observed for ribonuclease A, confirming that protein−displacer binding is responsible for the selectivity in these systems. This work demonstrates the utility of fluorescent displacers to enable online monitoring of displacer breakthroughs while also acting as efficient displacers for protein purification.

Introduction

Displacement chromatography is a powerful separation technique that enables the simultaneous concentration and purification of biomolecules from complex mixtures in a single step.[1] Displacement chromatography has been successfully employed for the purification of proteins using hydroxyapatite,[2,3] hydrophobic interaction,[4] and ion exchange chromatographic systems.[5−16] In particular, ion exchange displacement chromatography has attracted significant attention as a powerful technique for the purification of biomolecules.[8,9,17] While previous work has employed high molecular weight displacers for protein purification in ion exchange systems,[2,3,10,18−21] our laboratory has been actively involved in the development of low molecular mass displacers.[8,13−17,22]

To add an orthogonal degree of separation to displacement chromatography, we have recently developed a modified

[†] Department of Chemical and Biological Engineering, Center for Biotechnology and Interdisciplinary Studies.
[‡] Department of Chemistry and Chemical Biology.
[§] Department of Biology, Center for Biotechnology and Interdisciplinary Studies.

(1) Frenz, J.; Horvath, C. *High-Perform. Liq. Chromatogr.* **1988**, *5*, 211–314.
(2) Vogt, S.; Freitag, R. *J. Chromatogr., A* **1997**, *760* (1), 125–137.
(3) Freitag, R.; Breier, J. *J. Chromatogr., A* **1995**, *691* (1), 101–112.
(4) Shukla, A. A.; Sunasara, K. M.; Rupp, R. G.; Cramer, S. M. *Biotechnol. Bioeng.* **2000**, *68* (6), 672–680.
(5) Barnthouse, K. A.; Trompeter, W.; Jones, R.; Inampudi, P.; Rupp, R.; Cramer, S. M. *J. Biotechnol.* **1998**, *66* (2−3), 125–136.
(6) Gerstner, J. A.; Morris, J.; Hunt, T.; Hamilton, R.; Afeyan, N. B. *J. Chromatogr., A* **1995**, *695* (2), 195–204.
(7) Shukla, A. A.; Hopfer, R. L.; Chakravarti, D. N.; Bortell, E.; Cramer, S. M. *Biotechnol. Prog.* **1998**, *14* (1), 92–101.
(8) Kundu, A.; Cramer, S. M. *Anal. Biochem.* **1997**, *248* (1), 111–116.
(9) Jayaraman, G.; Gadam, S. D.; Cramer, S. M. *J. Chromatogr., A* **1993**, *630* (1−2), 53–68.
(10) Peterson, E. A.; Torres, A. R. *Anal. Biochem.* **1983**, *130* (1), 271–282.
(11) Jayaraman, G.; Li, Y. F.; Moore, J. A.; Cramer, S. M. *J. Chromatogr., A* **1995**, *702* (1−2), 143–155.
(12) Barnthouse, K. A.; Trompeter, W.; Jones, R.; Inampudi, P.; Rupp, R.; Cramer, S. M. *J. Biotechnol.* **1998**, *66* (2−3), 125–136.
(13) Shukla, A. A.; Deshmukh, R. R.; Moore, J. A.; Cramer, S. M. *Biotechnol. Prog.* **2000**, *16* (6), 1064–1070.
(14) Tugcu, N.; Deshmukh, R. R.; Sanghvi, Y. S.; Moore, J. A.; Cramer, S. M. *J. Chromatogr., A* **2001**, *923* (1−2), 65–73.
(15) Rege, K.; Ladiwala, A.; Cramer, S. M. *Anal. Chem.* **2005**, *77*, 6818–27.
(16) Rege, K.; Hu, S.; Moore, J. A.; Dordick, J. S.; Cramer, S. M. *J. Am. Chem. Soc.* **2004**, *126* (39), 12306–12315.
(17) Tugcu, N.; Deshmukh, R. R.; Sanghvi, Y. S.; Cramer, S. M. *React. Funct. Polym.* **2003**, *54* (1−3), 37–47.
(18) Antia, F. D.; Fellegvari, I.; Horvath, C. *Ind. Eng. Chem. Res.* **1995**, *34* (8), 2796–804.
(19) Frenz, J.; Horvath, C. *High-Perform. Liq. Chromatogr.* **1998**, *5*, 211–314.
(20) Vogt, S.; Freitag, R. *Biotechnol. Prog.* **1998**, *14* (5), 742–748.
(21) Schmidt, B.; Wandrey, C.; Freitag, R. *J. Chromatogr., A* **2002**, *944* (1−2), 149–159.
(22) Gallant, S. R.; Cramer, S. M. *J. Chromatogr., A* **1997**, *771* (1−2), 9–22.
(23) Tugcu, N.; Ladiwala, A.; Breneman, C. M.; Cramer, S. M. *Anal. Chem.* **2003**, *75*, 5806–16.

technique, namely, chemically selective displacement.[24,25] In this technique, certain biomolecules are selectively "retained" behind the displacer front. In a recent study, saturation transfer difference (STD) NMR[26] was employed to investigate binding events between chemically selective displacers and proteins.[27] This technique takes advantage of intraprotein spin diffusion, intermolecular dipolar coupling mechanisms, and ligand exchange between the bound and free states to characterize binding interactions. In that study it was directly verified that chemically selective displacement occurs by a selective binding between the displacer and protein. From this mechanism selective displacers are able to be designed rationally on the basis of the combination of a protein binding affinity and a resin binding affinity.

A robotic high-throughput screening has also been carried out to identify and characterize a large set of cationic chemically selective displacers.[28] From that study several compounds were identified as being both selective and exclusive in separating multiple protein mixtures. Trends in chemical moieties of selective displacers from this study indicated that selective displacers contained distinct hydrophobic regions, indicating that protein−displacer binding via hydrophobic interactions may be playing a role in these systems.

One of the major impediments to the implementation of displacement chromatography is the need to collect fractions from the column effluent for time-consuming offline analysis. The ability to employ direct online monitoring of displacement chromatography would have significant implications for applications ranging from analytical to preparative protein separations. In this work we use the known mechanism and structures of chemically selective displacers to design different fluorescent, chemically selective displacers to enable direct, online monitoring of the displacement separation. Chosen fluorescent cores are functionalized into displacers using different, known resin-binding functional groups. DC-50 and selectivity pathway plots[28,29] from batch experiments and column displacements are used to determine the separation performance of these new fluorescent displacers. Finally, STD-NMR is employed to study the binding between the new fluorescent displacers and proteins.

Experimental Section

Materials. SP Sepharose HP bulk resin and Pharmacia empty glass columns (4.6 mm × 100 mm) were purchased from GE Healthcare (Uppsala, Sweden). Ninety-six-well Multiscreen-HV Durapore membrane bottomed plates were purchased from Millipore (Bedford, MA). A Jupiter 5 μm C4 300A column (4.6 mm × 50 mm) was purchased from Phenomenex (Torrance, CA). Ribonuclease A (RNaseA), α-chymotrypsinogen A (α-ChyA), horse cytochrome *c* (Cyt*c*), lysozyme (Lys), sodium phosphate (monobasic and dibasic), acetonitrile (ACN), trifluoroacetic acid (TFA), acetic acid (glacial), sodium acetate, sodium chloride, hydrochloric acid, sodium hydroxide, trizma acid, trizma base, diethylenetriamine, ethylenediamine, and 2-amino-5-(diethylamino)pentane were purchased from Sigma-Aldrich (St. Louis, MO). Dansyl chloride and tris(2-aminoethyl)amine were purchased from Fluka (Seelze, Germany). NMR sample tubes, 5 mm thin wall, 600 MHz, were purchased from Wilmad Laboratory Glass (Buena, NJ). Deuterium oxide (99.96% purity) was purchased from Cambridge Isotope Laboratories, Inc. (Andover, MA). All other unlisted chemicals were obtained from Sigma-Aldrich. All reagents and solvents were used as received without further purification.

Equipment. A Buchi Rotavapor (Flawil, Switzerland) and a Napco vacuum oven (Waltham, MA) were used for chemical synthesis. NMR spectra for the determination of product purity and validation were obtained using a Varian Unity 500 NMR spectrometer (Palo Alto, CA). MS spectra were obtained using an Agilent 1100 series LC/MSD-SL ion trap system (Santa Clara, CA). Instrument control, data acquisition, and data processing were performed on these machines using ChemStation 10.01 and Ion Trap 5.2 software from Agilent. High-throughput batch screening experiments were carried out on a Biomek 2000 robotic liquid handling system from Beckman Coulter (Fullerton, CA). Supernatant solution was collected from the membrane plates using a vacuum manifold donated by Millipore. Supernatant solution analysis and column separations were carried out on an HPLC system consisting of a 600E HPLC pump and controller, a 712 WISP autoinjector, and a 484 absorbance detector from Waters (Milford, MA). The HPLC system utilized Millennium v.2.15.01 software for data acquisition, also from Waters. Fractions from the column runs were collected using an Advantec SF-2120 autosampler (Tokyo, Japan). Freeze-drying of NMR samples was done on a Labconco freeze-dry system from Labconco (Kansas City, MO). STD-NMR spectra were obtained using a Bruker 600 MHz spectrometer equipped with a cryogenically cooled 5 mm triple-resonance probe head with *z*-axis gradients (Billerica, MA). NMR data acquisition and analysis was carried out using the Topsin 2.1 software package, also from Bruker.

Procedures. 1. Product Characterization. ^{1}H and ^{13}C NMR spectral data were collected using the Varian Unity 500 NMR spectrometer. The sample solutions were prepared in $CDCl_3$ and D_2O and were referenced in parts per million relative to 7.27 ppm and 4.8 ppm each for ^{1}H NMR. Electrospray ionization mass spectrometry (ESI-MS) spectra were obtained for the sample solutions using the Agilent 1100 series LC/MSD-SL ion trap system. Samples were introduced into the ion source using a syringe pump at a flow rate of around 7 μL/min or by using an autosampler with a solvent flow rate of 200 μL/min. Data were collected in the positive ion mode. Data processing was then performed using the ChemStation 10.01 and IonTrap 5.2 software.

2. High-Throughput Batch Screen of Fluorescent Displacers. A robotic HTS protocol that had been previously developed was used to determine the performance of the fluorescent displacers.[28] The bulk stationary phase (SP Sepharose HP) was first washed twice with deionized water and then twice with the appropriate buffer and was allowed to equilibrate for 3 h between each wash. Buffers for the batch displacement runs were as follows: RNaseA and α-ChyA, 50 mM sodium phosphate at pH 6; Cyt*c* and Lys, 50 mM sodium acetate at pH 5.

After gravity settling of the stationary phase, the supernatant liquid was removed and 1.3 mL of the remaining stationary phase slurry was equilibrated with 15.6 mL of protein mixture at a total protein concentration of 5 mg/mL (2.5 mg/mL RNaseA and α-ChyA each or Cyt*c* and Lys each). The protein solution was equilibrated with the resin for 10 h, during which the stationary phase was allowed to settle under gravity. Upon settling, the supernatant liquid was removed, and the protein content in the supernatant solution was determined by reversed-phase liquid chromatography (RPLC) analysis (see below). The mass of the protein adsorbed on the stationary phase was then calculated by mass balance.

The protein-saturated resin was than resuspended as a 50:50 (v/v) slurry using some of the previously removed supernatant from the protein loading step (to prevent any desorption), and the resin slurry was loaded into a reservoir on the robotic liquid handler

(24) Tugcu, N.; Cramer, S. M. *J. Chromatogr., A* **2005**, *1063* (1−2), 15–23.
(25) Mayer, M.; Meyer, B. *J. Am. Chem. Soc.* **2001**, *123*, 6108–6117.
(26) Morrison, C. J.; Godawat, R.; McCallum, S. A.; Garde, S.; Cramer, S. M. *Biotechnol. Bioeng.*, accepted for publication.
(27) Morrison, C. J.; Cramer, S. M. *Biotechnol. Prog.*, accepted for publication.
(28) Rege, K.; Tugcu, N.; Cramer, S. M. *Sep. Sci. Technol.* **2003**, *38* (7), 1499–1517.
(29) Rule G. S.; Hitchens, T. K. *Fundamentals of Protein NMR Spectroscopy*; Springer: Dordrecht, The Netherlands, 2006.

(Biomek). In addition, 10 mM solutions of each displacer (in the appropriate buffer) were loaded into separate reservoirs, and the buffer was loaded into its own reservoir. A premade protocol was then employed to run the batch screen. The Biomek dispensed 20 μL of the resin slurry into each well of a 96-well membrane plate; the resin slurry reservoir was mixed before each aspiration. Once the liquid from the slurry was placed in each well, a vacuum manifold was used to filter the slurries through the membrane plate, leaving 10 μL of settled resin in each well. The Biomek performed serial dilutions of each displacer and then dispensed 120 μL of 10, 9, 8, 6, 5, 4, 2, and 1 mM displacer solutions into each individual well. Each displacer concentration was done in triplicate. After all solutions were loaded into the wells, the suspensions were mixed by repeated pipetting and allowed to equilibrate for 3 h and then mixed again and allowed to equilibrate for an additional 2 h. After the final equilibration the supernatant solutions from the wells were collected for analysis using the vacuum manifold.

3. Analysis of the Batch Supernatant Solutions. The batch supernatant solutions were analyzed using RPLC. RPLC was carried out using a C4 column (50 × 4.6 mm) with an A buffer of deionized water with 0.1% TFA and a B buffer of 90% ACN, 10% deionized water, and 0.1% TFA (all by volume). The column was first pre-equilibrated with 20% B. A linear gradient was then carried out from 20% to 100% B in 10 column volumes followed by 100% B for 2.5 column volumes. The flow rate was 1 mL/min, the column effluent was monitored at 280 nm, and 40 μL portions of the supernatant solutions were injected. This protocol resulted in the flow through of the displacers and the elution of the proteins during the linear gradient.

4. Fluorescent Column Displacements. For the displacement experiments a SP Sepharose HP column (100 mm × 4.6 mm i.d.) was initially equilibrated with the appropriate carrier buffer (50 mM sodium phosphate, pH 6 for α-ChyA/RNaseA and 50 mM sodium acetate, pH 5 for Cyt*c*/Lys). The column was then perfused sequentially with feed, displacer, and regeneration solutions. The experimental conditions, such as feed load, flow rate, and displacer concentration can be found in the figure captions. Regeneration was carried out using a linear gradient from the carrier buffer to the regeneration buffer (50 mM Tris, pH 10 with 2 M sodium chloride). (Note: the efficacy of this regeneration protocol was found to be effective at removing all of the bound displacers.) Fractions of the column effluent (200 μL) were collected during the displacement experiment for subsequent analysis. The column effluent was monitored by both UV (280 nm) and fluorescence (excitation 383 nm, emission 553 nm).

5. Analysis of the Column Effluent Fractions. After the fractions were collected, they were analyzed using RPLC. RPLC was carried out using the same column and buffers as described for the analysis of the batch experiments. The column was first pre-equilibrated with 100% A. A linear gradient was then carried out from 0 to 100% B in 20 column volumes followed by 100% B for 2.5 column volumes. The flow rate was 1 mL/min, the column effluent was monitored by both UV (280 nm) and fluorescence (excitation 383 nm, emission 553 nm), and 40 μL portions of the fractions were injected. This protocol resulted in the elution of both the displacer and proteins during the linear gradient. The protein amounts were determined by the UV readings, while the displacer amounts were determined by the fluorescence readings.

6. STD-NMR Sample Preparation and Experimental Protocol. Protein and displacer stock solutions for NMR analysis were first suspended in 50 mM sodium phosphate buffer at pH 6. The solutions were pH adjusted to ensure a pH of 6.0 and then lyophilized. The resulting pellets were suspended in deuterium oxide and lyophilized twice for two cycles before a final suspension was made in deuterium oxide. Actual NMR samples were prepared by diluting the stock solutions to their final analysis concentrations (10 mM for displacers and 0.2 mM for proteins) in D_2O-based buffer and were then placed in the NMR sample tubes.

Samples were analyzed using the STD method discussed in the Introduction. This protocol is described in detail elsewhere[26] and will be briefly summarized here. In this study the methyl protons within the protein were directly irradiated using a train of highly selective RF pulses, such that ligand (displacer) resonances were not directly perturbed. The extended saturation period provided by the RF pulse train permitted spin diffusion to spread the saturation of methyl proton magnetization to all protons throughout the entire protein. However, ligand protons near the protein surface (<5 Å) also experienced the saturation effect due to intermolecular dipolar coupling. Transfer of magnetization from the protein to the ligand resulted in an increase in signal intensity for ligand protons at the protein interaction surface relative to those distant. A control spectrum was used where the RF irradiation was applied to a spectral region devoid of ligand and protein resonances. The final STD spectrum was obtained after subtraction of the control from the experimental spectra. Ligand exchange between the bound and free states during this saturation period is also a key element of this technique and permitted measurement of the STD perturbations in the free ligand. Ligand concentrations were present in excess relative to the protein to ensure that saturated ligand remained in the unbound state for detection. A filter was also applied to remove the protein signal, thus leaving only a spectrum of ligand resonances that underwent an STD effect.

Mixtures of 50:1 (10 mM:0.2 mM) of displacer and protein, respectively, were analyzed utilizing the experimental parameters stated below. Additional control STD spectra were acquired on individual displacer and protein samples of the same concentration analyzed in the mixtures. A saturation period of 2.4 s was applied as a train of 8 ms Gaussian pulses applied at 40 ms intervals with a 50 Hz $\mathbf{B}_1$ field. The experimental and control spectra were acquired in an interleaved fashion with the saturating frequency centered at −0.25 and −10 ppm, respectively. Spectra were acquired using a 2 s acquisition time with a total of 1024 scans. An 80 ms T1rho filter was used to remove residual signal from the protein. Resonance assignments for displacers CBZEHTA, DEDA, and DTAEA were obtained by analyzing 2D $^1H-^{13}C$ HSQC, $^1H-^1H$ TOCSY, COSY, and NOESY spectra.[30]

Displacer Synthesis. 1. Synthesis of Dansyl-Based Cationic Displacers (Scheme 1). 1.1. DEDA·HCl (DEDA). To excess ethylenediamine (12 mL) was added dropwise dansyl chloride (1.50 g, 5.56 mmol) in methylene chloride at 0 °C under nitrogen over 30 min. The reaction mixture was stirred overnight with the reaction temperature steadily increasing to room temperature. A saturated aqueous solution of sodium carbonate was added to the reaction mixture with stirring. The organic layer was extracted with methylene chloride and then washed three times with water. The combined organic layer was then dried with Na_2CO_3. Solvent was removed using a Rotavapor. The resulting viscous product was further purified by recrystallization from a mixture of methylene chloride, toluene, and *n*-hexane in a ratio of 1:6:0.5, respectively. The resulting solid was obtained by filtration and dried in a vacuum oven overnight, yielding a yellow solid. The product (1.00 g, 3.40 mmol) was dissolved in methylene chloride and acidified with HCl gas for 12 h. The formed precipitate was filtered, dissolved in a small amount of water, and acidified further by addition of 2 mL of HCl (aqueous, 37%). The solution was then filtered and dried in a vacuum oven. After the resulting solid was washed with acetone, it was again dried in a vacuum oven to give a yellow solid final product, DEDA·HCl (0.90 g, 72% yield): ^1H NMR (500 MHz, D_2O) δ 8.63 (d, 1H), 8.42 (d, 1H), 8.30 (d, 1H), 8.50 (d, 1H), 7.85 (m, 2H), 3.45 (s, 6H), 3.10 (m, 4H); ^{13}C NMR (500 MHz, D_2O) δ 139.24, 134.53, 130.81, 128.76, 128.51, 127.08, 126.35, 126.22, 126.05, 119.69, 46.97, 40.05, 39.46; ESI-MS (*m*/*z*) for $C_{14}H_{19}N_3O_2S$ $[MH]^+$ calcd 294.12, found 294.0.

(30) ChemAxon. Marvin Calculator and Plugin, 2008. http://www.chemaxon.com/marvin/sketch/index.html.

Scheme 1

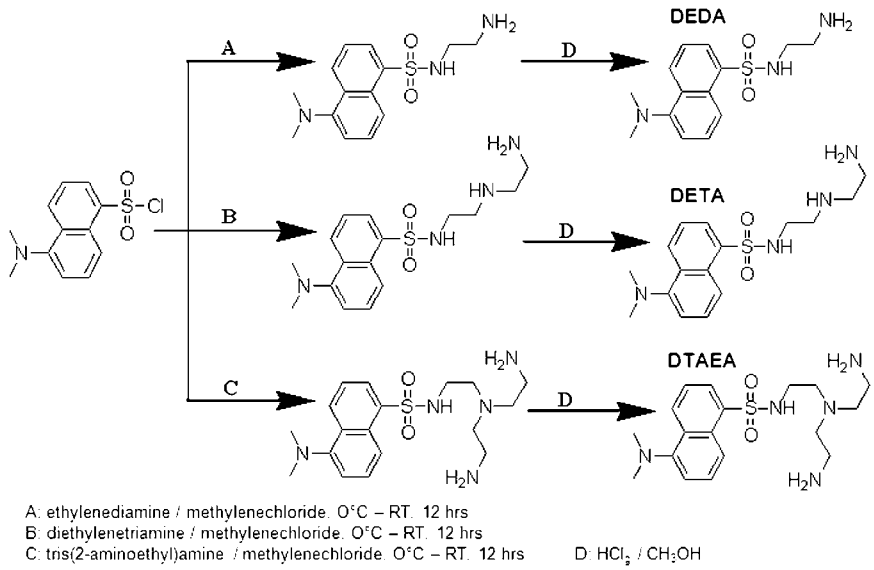

Scheme 2

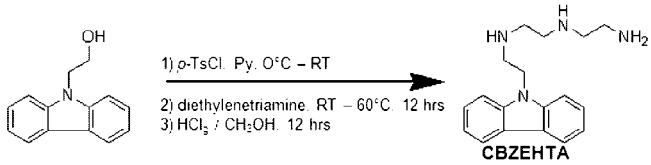

1.2. DETA·HCl (DETA). The reaction procedure was identical to the synthetic procedure of DEDA·HCl except for using diethylenetriamine (15 mL) instead of ethylenediamine: yield 0.91 g (68%); ^{1}H NMR (500 MHz, D_2O) δ 8.79 (d, 1H), 8.53 (d, 1H), 8.43 (d, 1H), 8.11 (d, 1H), 7.95 (m, 2H), 3.53 (m, 10H), 3.49−3.28 (m, 4H); ^{13}C NMR (500 MHz, D_2O) δ 139.17, 134.37, 130.86, 128.78, 128.55, 127.06, 126.44, 126.22, 126.05, 119.73, 47.85, 46.94, 44.47, 39.05, 35.57; ESI-MS (*m*/*z*) for $C_{16}H_{24}N_4O_2S$ $[MH]^+$ calcd 337.17, found 337.10.

1.3. DTAEA·HCl (DTAEA). The reaction procedure was identical to the synthetic procedure of DEDA·HCl except for using tris(2-aminoethyl)amine (15 mL) instead of ethylenediamine: yield 1.00 g (72%); ^{1}H NMR (500 MHz, D_2O) δ 8.75 (d, 1H), 8.45 (d, 1H), 8.39 (d, 1H), 8.16 (m, 1H), 7.90 (m, 2H), 3.53 (s, 6H), 3.33−3.20 (m, 8H), 3.19−3.10 (m, 4H); ^{13}C NMR (500 MHz, D_2O) δ 138.57, 134.19, 131.00, 128.60, 128.45, 127.16, 126.48, 126.21, 125.78, 119.83, 52.88, 50.28, 47.01, 38.59, 35.09; ESI-MS (*m*/*z*) for $C_{18}H_{29}N_5O_2S$ $[MH]^+$ calcd 380.20, found 380.20.

2. Synthesis of a Carbazole-Based Cationic Displacer (Scheme 2). 2.1. Tosylated Carbazole. A solution of 9*H*-carbazole-9-ethanol (5.00 g, 23.70 mmol) in pyridine (40 mL) was added dropwise to a solution of *p*-toluenesulfonyl chloride (6.70 g, 35.50 mmol) also in pyridine (40 mL) at room temperature under nitrogen. The reaction mixture was stirred overnight. The suspension was then poured into ice−water with stirring, resulting in a sticky product. The resulting product was then washed five times with water and dissolved in acetone. Water was then slowly added dropwise to the solution, yielding a white precipitate. After the solid was filtered and dried in a vacuum oven, it was washed with diethyl ether and redried in a vacuum oven over phosphorus pentoxide overnight, resulting in a white solid final product: yield 5.70 g (66%); ^{1}H NMR (500 MHz, D_2O) δ 8.01 (d, 2H), 7.41 (t, 2H), 7.25−7.20 (m, 6H), 6.84 (d, 2H), 4.52 (t, 2H), 4.41 (t, 2H), 2.25 (s, 3H).

2.2. CBZEtEDA·HCl (CBZEHTA). The tosylated carbazole (1.00 g, 2.74 mmol) and diethylenetriamine (15 mL) were placed in a round-bottom flask under nitrogen. The reaction mixture was stirred for 6 h at room temperature and then heated for 6 h at 60 °C. After the solution was cooled to room temperature, an aqueous sodium carbonate solution (20%) was added with stirring. The solution was then extracted with methylene chloride, washed five times with water, dried over sodium sulfate, and filtered. The solvent was removed using a Rotavapor. The resulting solid was then dried in a vacuum oven overnight, yielding a yellow solid. The sticky product was further purified by precipitation from diethyl ether and carbon tetrachloride. The resulting product was dried in a vacuum overnight at 40 °C. The obtained product (1.00 g, 3.95 mmol) was acidified in methanol (30 mL) with HCl gas for 12 h in an ice−water bath. The precipitate was filtered and washed with chloroform, methanol, and acetone. The obtained solid was dried in a vacuum oven overnight to give CBZEHTA·HCl: yield 0.86 g (58%); ^{1}H NMR (500 MHz, D_2O) δ 8.16 (d, 2H), 7.52 (m, 4H), 7.31 (t, 2H), 4.63 (t, 2H), 3.63 (t, 2H), 3.41−3.34 (m, 8H); ^{13}C NMR (500 MHz, D_2O) δ 139.85, 126.54, 122.80, 120.71, 120.00, 108.84, 46.76, 44.57, 43.71, 43.46, 39.08, 35.38; ESI-MS (*m*/*z*) for $C_{18}H_{24}N_4$ $[MH]^+$ calcd 297.20, found 297.20.

Results and Discussion

As stated in the Introduction, there is a significant need for the development of displacers which would permit direct online monitoring of displacement chromatographic processes. Further, the ability to design chemically selective displacers that enabled online monitoring would be particularly advantageous. Previous work in our laboratory has identified a double aromatic ring head and a positively charged amine tail as important structural motifs for chemically selective displacers on a strong cation exchange resin.[28] Accordingly, the fluorescent displacers in the current work were designed to incorporate these motifs. Carbazole and dansyl chloride were chosen as building blocks because of their fluorescent nature, exposed double aromatic ring structure, low cost, and ease of chemical modification. These building blocks were then functionalized with amine tails of various lengths and charges (which would interact with the resin) as described in the Experimental Section, creating a homologous library of fluorescent displacers.

The four fluorescent displacers synthesized as described in Schemes 1 and 2 are presented in Figure 1. The individual amine pK_a values were determined for these displacers using the

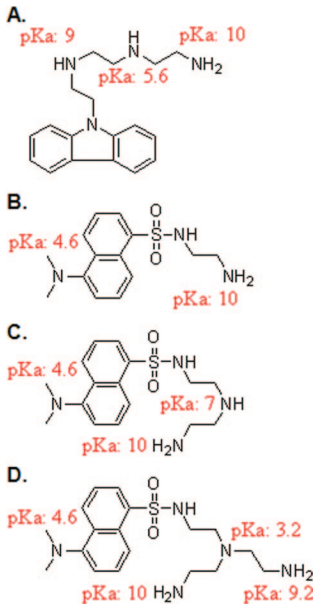

Figure 1. Amine pK_a values for the fluorescent displacers: (A) CBZEHTA, (B) DEDA, (C) DETA, (D) DTAEA.

Table 1. Net Molecular Charge of the Fluorescent Displacers at the Experimental pH Values

displacer	pH 6.0	pH 5.0
CBZEHTA	+2.25	+2.75
DEDA	+1	+1.25
DETA	+1.75	+2.2
DTAEA	+2	+2.75

ChemAxon Marvin Calculator[31] and are indicated in the figure. These values were then used to determine the overall molecular charge of the displacers at the experimental pH values and are given in Table 1. As seen in the table, the amount of charge varied between the different displacers, with DEDA having the least amount of charge and CBZEHTA possessing the highest amount of charge. Because the aromatic portion of these molecules stays constant (the dansyl chloride-derived molecules) while the amount of charge varies, any differences in displacement behavior between the displacers can most likely be attributed to the difference in charge and charge distribution. While CBZEHTA had its charge concentrated on the amine tail, the three dansyl chloride-derived displacers had charge on both the amine tail and the other side of the molecule at pH 5.

Batch Experiments with Fluorescent Displacers. To investigate the performance of these compounds, a robotic high-throughput batch screen previously developed in our laboratory was employed. In this screen the resin was loaded with equal amounts of each protein from a model protein pair to determine the displacer's efficacy in a multicomponent mixture. (Note: the proteins in each protein pair exhibited very similar retention times in linear gradient chromatography under the same pH and column conditions.[28]) These batch experiments were carried out at several displacer concentrations, and the results were used to generate DC-50 plots and selectivity pathway plots[28,29] for the displacer compounds (Figures 2 and 3). DC-50 plots present data for the percentage of protein displaced in batch experiments as a function of the displacer concentration. In selectivity pathway plots, the percentage of one protein displaced from a pair is plotted as a function of the percentage of the other displaced protein in the pair. The trajectory is then constructed at increasing displacer concentrations and different regions of the plot are defined.

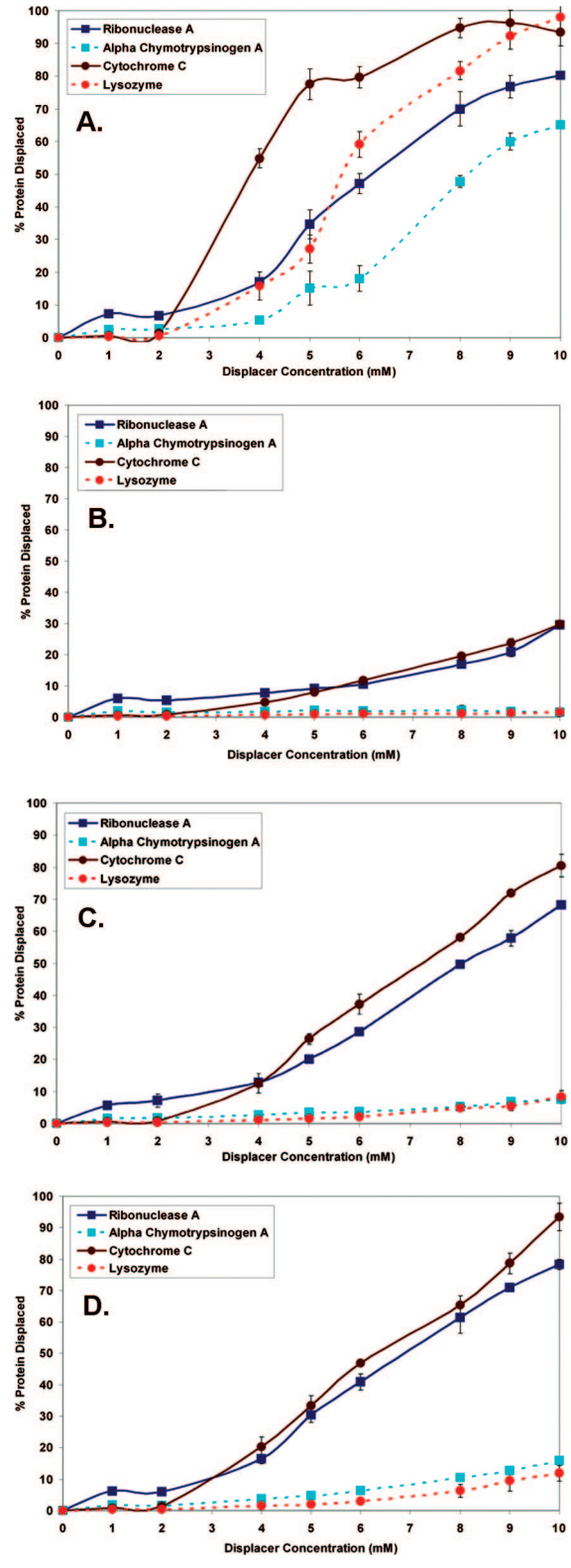

Figure 2. DC-50 plots of the fluorescent displacers for the protein pairs α-ChyA/RNaseA and Cytc/Lys: (A) CBZEHTA, (B) DEDA, (C) DETA, (D) DTAEA. The given error bars represent ±1 standard deviation of the triplicate values.

(31) Liu, J.; Hilton, Z. A.; Cramer, S. M. *Anal. Chem.* **2008**, *80* (9), 3357–3364.

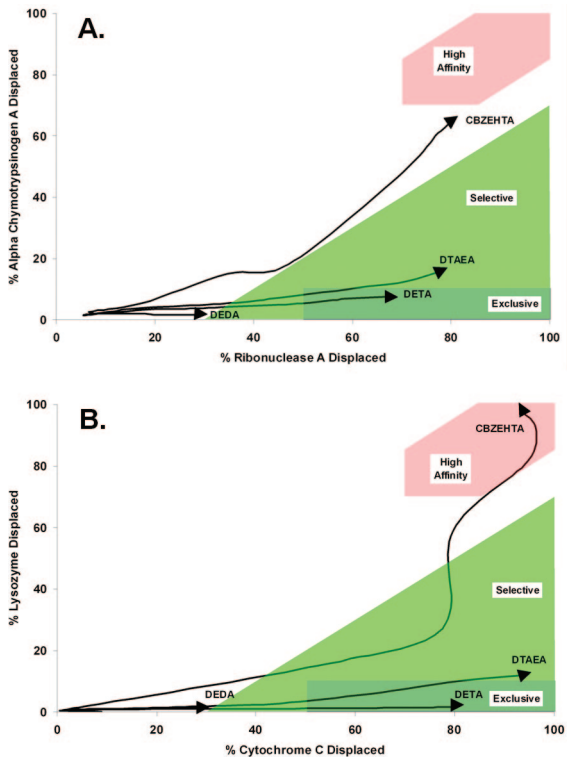

Figure 3. Selectivity pathway plots of the fluorescent displacers for the two protein pairs: (A) α-ChyA/RNaseA, (B) Cyt*c*/Lys.

As can be seen in Figure 2A the carbazole-derived fluorescent displacer, CBZEHTA, did not give a selective separation between the proteins of each pair. In fact, at higher concentrations this displacer behaves as a high-affinity displacer rather than a selective one. This result was unexpected because the design of CBZEHTA fits the standard design of a chemically selective displacer for these protein pairs, namely, a double aromatic ring head with a positively charged amine tail. However, in our previous work,[28] it was established that the design of a chemically selective displacer is a delicate balance between the displacer's affinity for the resin and its affinity for binding to the "selected protein", in this case α-ChyA or Lys. It is believed that the nonselective result shown with CBZEHTA was caused by too much charge being present on the amine tail, a total of 2.25 and 2.75 positive charges at the experimental conditions of pH 5 and 6, respectively. In addition, as indicated above, all of this charge was located on the amine tail. This higher charge density makes the CBZEHTA more efficient at displacing proteins from the resin, thus not enabling efficient selective displacement to take place. This hypothesis is supported by Figure 3B, where CBZEHTA acts as a selective displacer for a specific range of concentrations. On the other hand, at higher displacer concentrations, this molecule acts as a fluorescent high-affinity displacer.

The plots shown in Figure 2B−D indicate the performance of the homologous series of dansyl chloride displacers. In Figure 2B, almost no α-ChyA or Lys is displaced while only a small amount of RNaseA or Cyt*c* is displaced. These results indicate that while DEDA might possess some selectivity for these protein pairs, the displacer has insufficient charge (+1 and +1.25 at pH 5 and 6, respectively) to displace proteins efficiently from the resin, making it an ineffective displacer.

The results with DETA are given in Figure 2C. As seen in the figure, while minimal α-ChyA or Lys was displaced, a large amount of the protein RNaseA or Cyt*c* was displaced in the batch experiments. These results indicate that DETA acts as an effective selective displacer, which is indicative of an appropriate balance of affinities for the resin and the selected protein. Because the only difference between DETA and DEDA (Scheme 1) is the amount of positive charge on the amine tails, it is clear that the latter did not possess sufficient charge to give a selective separation.

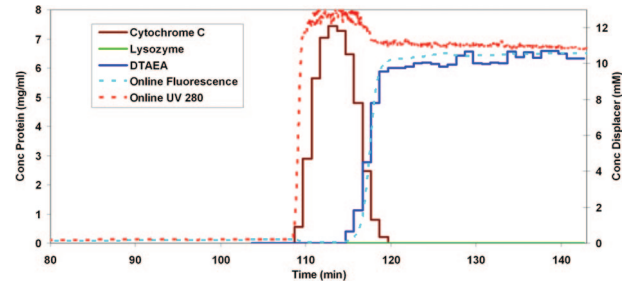

Figure 4. Selective displacement of the Cyt*c*/Lys protein pair using 10 mM DTAEA: column, 100 mm × 4.6 mm i.d., HP Seph SP resin; carrier, 50 mM sodium acetate buffer, pH 5.0; protein loading, 10 mg each of Cyt*c* and Lys; flow rate, 0.2 mL/min; online UV, 280 nm; online fluorescence, excitation 383 nm, emission 553 nm.

The results for DTAEA, which has slightly more charge than DETA (Table 1), are given in Figure 2D. As seen in the figure, DTAEA also acted as an efficient selective displacer for both protein pairs. While the performances of DETA and DTAEA were similar, DTAEA was slightly more efficient at displacing the proteins, in general.

It is instructive to evaluate the selectivity pathway plots for the homologous series of dansyl chloride displacers, Figure 3. As seen in the figure, DEDA was unable to give a selective separation at the concentrations evaluated, most likely due to insufficient charge. On the other hand, DETA, with an increased amount of charge, gave not only a selective separation but an exclusive separation[27] (where there is a greater than 50% separation in the pair and one protein remains strongly bound onto the resin with less than 10% displaced) at certain concentrations as well. While DTAEA also produced exclusive separations, the concentration range of exclusivity was more limited than for DETA. From these data it is clear that the dansyl chloride-derived displacers are indeed selective. In fact, DETA and DTAEA have actually exhibited some of the best batch experiment separations of any chemically selective displacer tested in our laboratory to date.[27,28,31]

Column Displacements using Fluorescent Displacers. One of the major challenges of displacement chromatography is the determination of the displacer breakthrough during column experiments. Typically, the breakthrough is determined by offline analysis of fractions from the column effluent, which is cumbersome and time-consuming. Accordingly, experiments were conducted to determine the performance of the fluorescent displacers in a column setting. In particular, it was desired to gauge the performance of the fluorescent displacers as a direct, online detection method in column displacement chromatography. The resulting selective column displacements of the two protein pairs Cyt*c*/Lys and α-ChyA/RNaseA are shown in Figures 4 and 5, respectively. Online detection methods (UV and fluorescence) are shown as thin dotted lines, while concentrations determined by fraction collection are shown as thick dark lines.

As can be seen in Figure 4, a complete separation between Cyt*c* and Lys was accomplished using 10 mM DTAEA as a

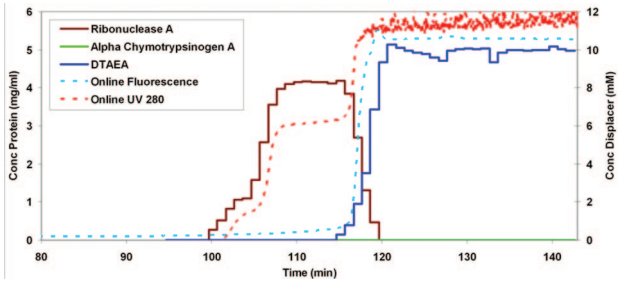

Figure 5. Selective displacement of the RNaseA/α-ChyA protein pair using 10 mM DTAEA: column, 100 mm × 4.6 mm i.d., HP Seph SP resin; carrier, 50 mM sodium phosphate buffer, pH 6.0; protein loading, 10 mg each of RNaseA and α-ChyA; flow rate, 0.2 mL/min; online UV, 280 nm; online fluorescence, excitation 383 nm, emission 553 nm.

displacer. Cytochrome *c* was completely displaced ahead of the displacement zone, as confirmed by mass balance, while no detectable amounts of Lys were seen in the fractions from the column effluent. This result demonstrates a complete separation of two components that directly overlapped under linear gradient ion exchange conditions. Importantly, when only the online detection methods are employed, significant information is provided regarding this two-protein displacement separation. The UV trace distinctly shows the protein zone ahead of the displacement front. while the fluorescence trace shows only the displacer breakthrough. Also, it can be seen that the online detection results directly reflect the results determined by fraction collection and offline analysis.

The selective column displacement of RNaseA/α-ChyA seen in Figure 5 indicates a result similar to that shown in Figure 4. Ribonuclease A was completely displaced ahead of the displacement zone, as confirmed by mass balance, while no detectable amounts of α-ChyA were seen in fractions from the column effluent. This result also demonstrates a complete separation of these two components. It is important to note these two proteins were inseparable under linear gradient ion exchange conditions carried out at the same pH. The small overlap between the displaced protein zones and the DTAEA zone in Figures 4 and 5 is comparable to that obtained previously with displacement chromatography on the SP Sepharose HP resin used. It should also be noted that no fluorescent signal quenching of the displacer by the proteins was seen in these column experiments. The results presented in Figures 4 and 5 provide proof of concept for the utility of online detection of separate protein and displacer zones in a column setting using fluorescent selective displacers.

STD-NMR Experiments on Fluorescent Displacers. Previous work done in our laboratory has shown that selective binding between a protein and displacer is the mechanism by which chemically selective displacement occurs.[27,28,31] STD-NMR experiments were employed to directly determine whether the fluorescent displacers bound selectively to proteins. Because the STD experiment can also give insight into where the binding occurs on the displacers at atomic resolution, proton peak assignments were also determined for the fluorescent displacers. These assignments were obtained using 2D NMR experiments (not shown) described in the Experimental Section using standard methodologies. Mixtures of a single protein and a single displacer in a 1:50 ratio were analyzed with the STD protocol. Solutions of the same concentration of protein and displacer were also analyzed as controls to verify the method and results. The resultant spectra from these experiments for CBZEHTA, DEDA, and DTAEA are shown in Figure 6. Proton peak assignments for the displacers are shown in the figure as well.

To simplify the discussion of the results in Figure 6, the spectra for each displacer will be evaluated in series. The proton peak assignments for the CBZEHTA displacer (A), shown on the left side of Figure 6, were made as follows: 6−1 on the amine tail and 10−7 on the aromatic rings (note that the peak for proton 6 is hidden in the water peak at 4.7 ppm). As can be seen from the STD spectra given in (B) and (C), a binding signal was clearly observed for the α-ChyA/CBZEHTA mixture while no signal was observed for the RNaseA mixture. Furthermore, a lack of signal from the single-component proteins (E, F) and single-displacer spectra (D) verified that any signal seen in the mixture experiments was caused by a binding event. Upon closer analysis of the α-ChyA/CBZEHTA mixture signal, it can be seen that the binding is centered on the aromatic portion of the displacer, with only a small amount of signal detected for protons within the amine tail, suggesting a hydrophobic binding event. This selective binding to α-ChyA for CBZEHTA was unexpected because the displacer gave a nonselective result from the analysis of the DC-50 plots. However, as stated previously, this nonselective result was most likely due to the differences in charge and charge distribution as compared to those of the other dansyl chloride-based displacers (Table 1). This makes the CBZEHTA more efficient at displacing proteins from the resin, thus not enabling efficient selective displacement to take place. If the amount of charge on CBZEHTA were reduced, a more selective result would most likely occur, as indicated by the selective binding event shown from the STD-NMR results.

The NMR results for the displacer DEDA are shown in the center of Figure 6. The proton peak assignments for this displacer (A) were made as follows: 1 and 2 on the amine tail, 3 on the aromatic ring ortho to the sulfone group with 4 meta and 5 para on the same ring, 6 on the dimethylamine off the other aromatic ring, and 7 on the aromatic ring ortho to the dimethylamine group with 8 meta and 9 para on the same ring. As can be seen from the STD spectra given in (B) and (C), a binding signal was clearly observed for the α-ChyA/DEDA mixture while the RNaseA mixture produced a relatively weak signal. The protein control experiments (E, F) showed no signal; however, a small amount of signal was seen in the STD spectrum of this displacer alone (D). This small residual STD signal is attributed to the direct saturation of the displacer, resulting in a slight amount of STD signal in the mixtures (B, C) as well as the control (D). If one compares the spectra in (B)−(D), it is clear that the signal obtained for the RNaseA mixture can be attributed primarily to the direct saturation of the displacer. In contrast, the signal obtained for the α-ChyA mixture is significantly higher than that of the displacer control, confirming displacer−protein binding. Upon closer analysis of the α-ChyA/DEDA mixture signal, it can be seen that the binding is centered on the aromatic portion of the displacer and the methyl groups of the dimethylamine group, while only a weak binding signal was seen for the amine tail. This would again suggest that the binding event is occurring primarily due to hydrophobic interactions. These NMR results indicate that DEDA binds selectively to α-ChyA while not binding to RNaseA, thus selectively displacing RNaseA while retaining α-ChyA on the resin surface, as indicated by the DC-50 plots. However, as shown in Figures 2 and 3, even though this displacer has some selectivity, it does not possess sufficient charge (Table 1) to efficiently displace any proteins from the resin, thus being categorized as an ineffective displacer.

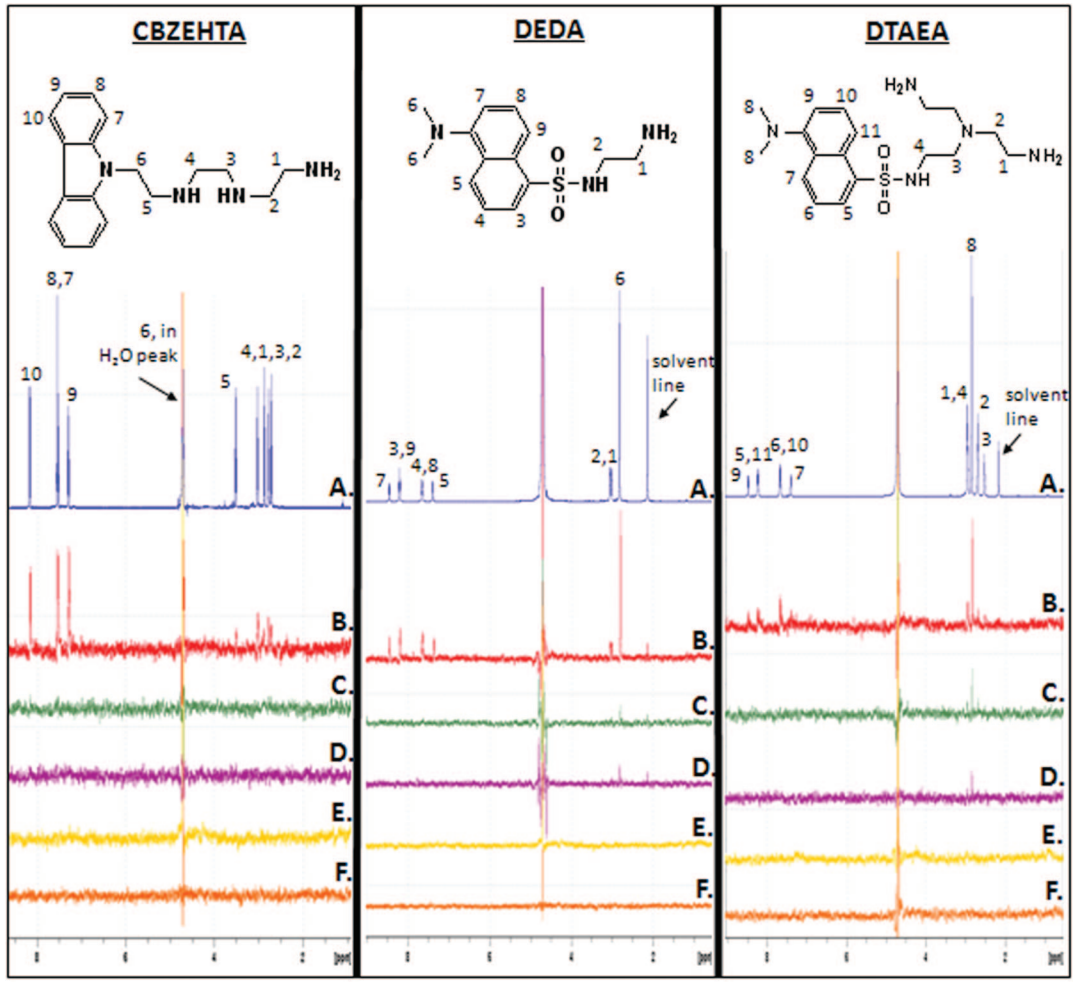

Figure 6. STD-NMR results for the protein/displacer experiments with proton peak assignments shown: (A) 1D proton spectra for the displacer (blue), (B) STD for the α-ChyA/displacer mixture (red), (C) STD for the RNaseA/displacer mixture (green), (D) STD control for the displacer (violet), (E) STD control for α-ChyA (yellow), (F) STD control for RNaseA (orange).

The NMR results for the displacer DTAEA are shown on the right side of Figure 6. The proton peak assignments for this displacer (A) were made as follows: 1 and 2 on the forked extension of the amine tail, 3 and 4 on the amine tail, 5 on the aromatic ring ortho to the sulfone group with 6 meta and 7 para on the same ring, 8 on the dimethylamine off the other aromatic ring, and 9 on the aromatic ring ortho to the dimethylamine group with 10 meta and 11 para on the same ring. As can be seen from the STD spectra given in (B) and (C), a binding signal was clearly observed for the α-ChyA/DTAEA mixture while the RNaseA mixture again produced a relatively weak signal. The protein control experiments (E, F) showed no signal; however, a small amount of signal was seen in the STD spectrum of this displacer alone (D). As with the DEDA results, if one compares the spectra in (B)−(D), it is clear that the signal obtained for the RNaseA mixture can be attributed primarily to the direct saturation of the displacer. In contrast, the signal obtained for the α-ChyA mixture is significantly higher than that of the displacer control, confirming displacer−protein binding. Upon closer analysis of the α-ChyA/DTAEA mixture signal, it can be seen that the binding is centered on the aromatic portion of the displacer and the methyl groups of the dimethylamine group, while only a weak binding signal was seen for the forked amine tail. This would also suggest that the binding event is occurring primarily due to hydrophobic interactions. These NMR results indicate that DTAEA binds selectively to α-ChyA while not binding to RNaseA, thus selectively displacing RNaseA while retaining α-ChyA on the resin surface, as indicated by the DC-50 plots.

The results from the STD-NMR confirm that all three of these displacers bind selectively to one of the proteins in each protein pair. However, as stated above, for the displacer to act as an effective selective displacer, it must both bind to one of the proteins and possess sufficient charge to displace the other protein from the resin surface. DEDA has too little charge and thus cannot effectively displace proteins. On the other hand, CBZEHTA has too much charge and displaces both proteins, even the one to which it binds. Finally, DTAEA has the appropriate balance between protein binding and resin affinity and can act as an efficient selective displacer for this specific class of separation problems, namely, the separation of proteins with similar ion exchange affinity but differing surface hydrophobicities.

Conclusion

This work has addressed one of the major obstacles to the widespread implementation of displacement chromatography, namely, the ability to carry out real time detection of the separation process. To address this challenge, fluorescent displacers were designed using known chemically selective displacers as templates. Fluorescent cores were chosen on the basis of their exposed aromatic ring structure, low cost, and

ease of chemical modification. The chosen cores were then functionalized with different charged moieties, creating a homologous library. These compounds were then tested on two protein pairs, α-ChyA/RNaseA and Cyt*c*/Lys, using batch and column displacement experiments. The batch results indicated that the fluorescent displacers acted as high-affinity, selective, or ineffective displacers depending on their charge. While the more charged fluorescent displacer CBZEHTA was generally found to be a nonselective, high-affinity displacer, two of the dansyl chloride-derived displacers, DETA and DTAEA, were highly selective and exclusive at multiple concentrations. Column displacements using 10 mM DTAEA yielded complete separation of both protein pairs while facilitating online detection using UV and fluorescence detection. STD-NMR was then carried out to investigate the binding of the fluorescent displacers to proteins. The NMR results indicated a selective binding of CBZEHTA, DEDA, and DTAEA to α-ChyA, while no binding was observed for RNaseA. These results indicate that if a molecule is to act as an effective selective displacer, it must bind to one of the proteins, while also possessing sufficient charge to displace the other protein from the resin surface.

This work demonstrates the ability to synthesize and employ fluorescent chemically selective displacers for protein purification. These displacers could be custom designed for different classes of protein separations using a similar methodology presented in this paper. The ability to directly monitor displacement separations online represents a significant advance in the field of displacement chromatography and promises to have a major impact on the implementation of this technology for applications ranging from the large-scale production of biopharmaceuticals to complex bench-scale bioseparations.

Acknowledgment. This work was partially supported by NIH Grant 5R01 GM047372 and NSF Grant CBET-0730830.

JA806279X